

# **MATERIAL PROPERTIES GOVERNING CO-CURRENT FLAME SPREAD: THE EFFECT OF AIR ENTRAINMENT**

**Mickael Coutin, Ali S. Rangwala, Jose L. Torero**

Department of Fire Protection Engineering, The University of Maryland  
College Park, MD20742, USA

**Steven G. Buckley**

Department of Mechanical Engineering, The University of Maryland  
College Park, MD20742, USA

## **ABSTRACT**

A study on the effects of lateral air entrainment on an upward spreading flame has been conducted. The fuel is a flat PMMA plate of constant length and thickness but variable width. Video images and surface temperatures have allowed establishing the progression of the pyrolysis front and on the flame stand-off distance. These measurements have been incorporated into a theoretical formulation to establish characteristic mass transfer numbers (“B” numbers). The mass transfer number is deemed as a material related parameter that could be used to assess the potential of a material to sustain co-current flame spread. The experimental results show that the theoretical formulation fails to describe heat exchange between the flame and the surface. The discrepancies seem to be associated to lateral air entrainment that lifts the flame off the surface and leads to an over estimation of the local mass transfer number. Particle Image Velocimetry (PIV) measurements are in the process of being acquired. These measurements are intended to provide insight on the effect of air entrainment on the flame stand-off distance. A brief description of the methodology to be followed is presented here.

## **INTRODUCTION**

The necessary flammability requirements for all materials to be used in space vehicles (NASA specifications) are given by the: “Flammability, Odor, Offgassing, and Compatibility Requirements and Test Procedures for Materials in Environments that Support Combustion” document [1]. This document specifies two tests that need to be performed before a material is qualified to be used in a space vehicle, the “Upward Flame Propagation Test” (Test 1) and the “Heat and Visible Smoke Release Rates Test” (Test 2). These two tests are expected to properly assess the flammability of a material in micro-gravity conditions. These two test methods attempt to provide a worst case scenario (Test 1) and a measure of the heat release (Test 2), and consequently, the “damage potential” of a fire. A detailed description of these test methods is provided in NASA-NHB 8060.1 [1] and an extensive list of the materials that have been tested is provided in the “Materials Selection List for Space Hardware Systems” [2].

The present study will address Test 1 and Test 2 in normal and micro-gravity to provide sound theoretical and experimental information that will serve to validate these methodologies and to help translate the results from normal-gravity to micro-gravity. The use of appropriate diagnostic techniques will help to accomplish these objectives.

Three fundamental parameters will be extracted as a combination of the results of Test 1 and Test 2 ( $B_A$ ,  $B_R$ ,  $B_C$ ). These parameters can be incorporated into fire growth models and used to bound the growth of a fire in micro-gravity due to co-current flame spread. Following this methodology the results are not only a “worst case scenario,” but a realistic representation of fire growth (through  $B_R$ ), bounded by a “worst case scenario” ( $B_A$ ) and a best case scenario ( $B_C$ ).

For risk assessment this information is essential. More details on the theory behind these mass transfer numbers are provided in reference [3].

## DESCRIPTION OF THE EXPERIMENTAL FACILITY

The experimental facility consists of a vertical sample of PMMA (0.45 m x 0.05 m (0.1 m and 0.15 m) x 0.012 m) mounted on an insulation board and covered with a metal plate (Figure 1). Tests were conducted with different arrangements for the edges to guarantee the most repeatable results. The sample was placed under a hood and ignition was induced with an electrically heated Kanthal wire. Five thermocouples were drilled from the back of the sample and melted on to the surface. Five thermocouples were placed at the back end of the sample between the fuel and the insulation. All thermocouples were spaced to provide a progression of the pyrolysis front and an estimate of the thermal thickness of the material. Two CCD cameras were used to obtain a frontal and a side view of the flame. Based on the characteristic times scales for propagation it was estimated that an average of all images covering a 10 second period was adequate to obtain an average stand-off distance and flame shape. Experiments were conducted with all three widths of the sample at least 5 times.

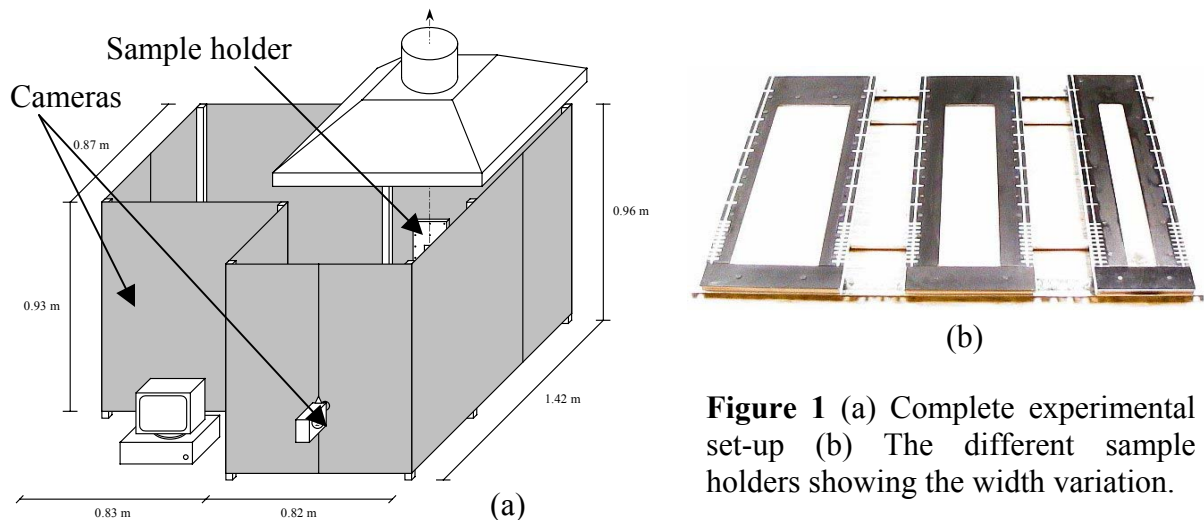


**Figure 1** (a) Complete experimental set-up (b) The different sample holders showing the width variation.

A PIV optical setup has been completed, including the optics to form the laser sheet and the image acquisition. The light sheet is placed perpendicular (and parallel) to the fuel surface and velocity measurements will be obtained at the edge of the flames. The location of the Laser sheet will be varied systematically to obtain a clear idea of the three-dimensional features of the flow. Several smoke generation techniques have been considered, including seeding with  $\text{TiO}_2$  particles, the use of a fog generator, and finally, the use of incense sticks. The  $\text{TiO}_2$  was rejected due to potential toxicity of the particles and the observed tendency of the particles to agglomerate. Attempts with a fog generator produced too much smoke, with the result that white particles settled throughout the laboratory. Currently incense sticks, which produce a light white smoke, are being tested.

## EXPERIMENTAL RESULTS

The progression of the pyrolysis front and the flame length was obtained from the thermocouple measurements and the video recordings. Figure 2 shows a characteristic set of data for a sample 0.05 m wide. As it can be seen the propagation rate and flame length seem to increase as a linear function of time. Other tests show similar relationships. It was noted that for

all cases studied the ratio between the flame pyrolysis lengths remains constant,  $L_F/L_P \approx 1.4$  with little scatter ( $\sigma < 0.2$ ). It is important to note that a single test provides a significant amount of data points, since the ratio can be evaluated at each stage of propagation. This ratio is much lower than earlier values reported by Orloff et al. (1974) who established  $L_F/L_P$  of the order of four. The reason for this is most likely consumption of fuel by lateral entrainment of air. The ratio  $L_F/L_P$  remained approximately the same for all sample width. This might indicate that lateral entrainment is not the cause for the flame length reduction but frontal views of the flame showed clearly that entrainment is dependent on the width and thus increases with this dimension. This compensates for the increased distance from the edges to the plane of symmetry.

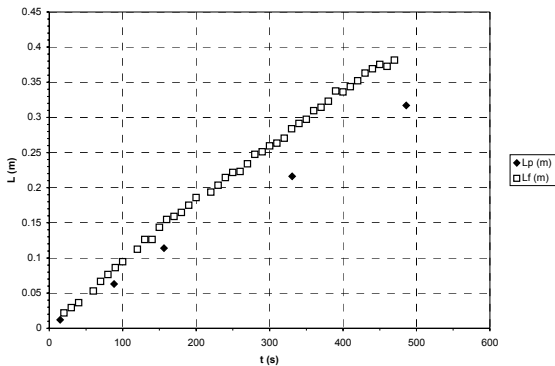


**Figure 2** Progression of the flame length ( $L_F$ ) and Pyrolysis length ( $L_P$ ) as a function of time.

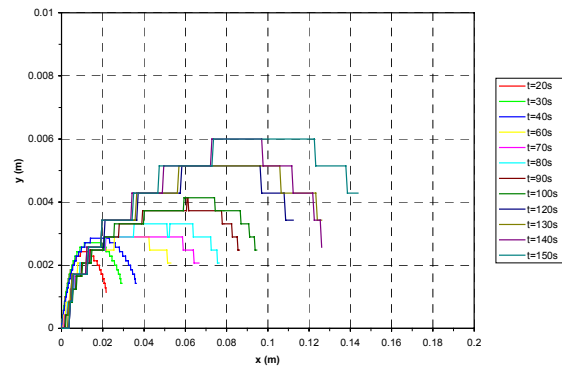


**Figure 3** Stand-off distance as a function of time and distance down stream from the leading edge.

Figure 3 shows the evolution of the stand-off distance with the stream wise coordinate “x.” As it can be seen as the flame length increases the stand-off distance increases. This is counter intuitive since an increase in flame length results in an increase in the characteristic length scale inducing natural convection and thus a thinner boundary layer (i.e. stand-off distance) should be expected. Fundamental theoretical studies of this type of flames will indicate that given a two-dimensional problem the stream wise length scales can be transformed by the following

expression  $\eta = (Gr_{L_F}^{1/4} / L_F \sqrt{2}) \int_0^y \frac{\rho}{\rho_\infty} dy$  where the Grashoff number is given by:

$Gr_x = \frac{gL_F^3 (T_w - T_\infty)}{v_\infty^2 T_\infty}$ , thus the flame length is the dominant parameter controlling natural convection [5].

Although the discrepancies with two-dimensional theory have been noted, it is useful to establish the theoretical stand-off distance as a function of the mass transfer number (“B” number). The analysis is the same as that reported by Annamalai and Sibulkin [5] and Pagni and Shih [6] so it will not be repeated here. Figure 4 shows the theoretical predictions for different values of the “B” number. Realistic mass transfer numbers for PMMA have been reported to be approximately 3 [6]. As can be observed from Figure 4, the stand-off distance increases with the mass transfer number. By matching the experimental stand-off distance with the theoretical predictions [3] the evolution of an empirical “B” number can be estimated. A set of these values has been presented in Figure 5. According to the theory, the stream wise coordinate should scale

with LP, thus all data should collapse to a single curve. This has been shown to be valid in micro-gravity by Torero et al. [3]. This is clearly not the case in normal gravity. Furthermore, the predicted values of the “B” number are much larger than those expected. An experimental over prediction of the stand-off distance will result in a significant increase in the mass transfer number. This again points towards lateral entrainment. Lateral entrainment lifts the flame away from the surface leading to much larger stand-off distances than those predicted by two dimensional theory. One final point to be made, the maximum value of the “B” number (i.e. stand-off distance) is achieved at the pyrolysis length, the reduction occurring downstream indicates the elimination of the fuel production for  $x > L_p$ . The “B” numbers presented in Figure 5 are thus only valid for  $x/L_p < 1$ , values downstream are only presented for illustration.

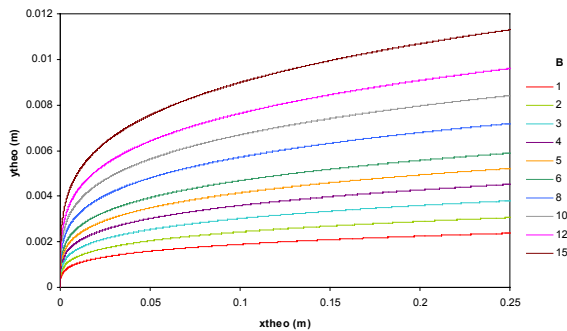


**Figure 4** Evolution of the theoretical stand-off distance with the “B” number.

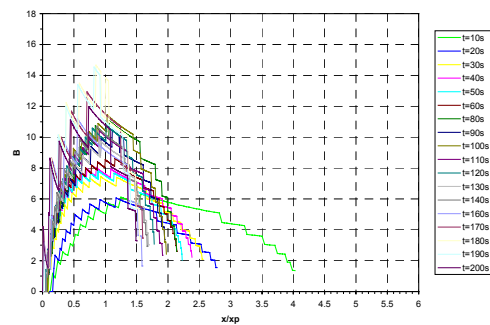


**Figure 3** Evolution of the empirical “B” number as a function of the normalized distance and time.

## CONCLUSIONS

A series of upward burning experiments have been conducted and have shown the importance of lateral entrainment in the establishment of the mass transfer number from flame stand-off distances. In micro-gravity gas expansion eliminates air entrainment and a two dimensional treatment is adequate. In normal gravity the lateral flow moves towards the plane of symmetry making impossible a two-dimensional treatment. Evaluation of these entrained flows using PIV and a numerical solution of the quasi-steady diffusion flames are the current tasks of this program.

## REFERENCES

1. “Flammability, Odor, Offgassing, and Compatibility Requirements and Test Procedures for Materials in Environments that Support Combustion” NASA-NHB 8060.1, 1981.
2. “Materials Selection List for Space Hardware Systems” MSFC-HDBK-527-REV F, September 30, 1988.
3. Torero, J.L., Vietoris, T., Legros, G., Joulain, P. “Estimation of a Total Mass Transfer Number from Stand-off Distance of a Spreading Flame,” *Combustion Science and Technology*, **174** (11-12), pp.187-203, 2002.
4. Orloff, L., De Ris, J. and Markstein, G.H. “Upward Turbulent Fire Spread and Burning of Fuel Surface,” *Fifteenth Symposium (International) on Combustion, The Combustion Institute*, 183-192, 1974.
5. Annamalai and Sibulkin, “Spread over Combustible Surfaces for Laminar Flow Systems, *Combustion Science and Technology*, v.19, pp.167-183, 1979.
6. Pagni P. J. and T. M. Shih, T.M., “Excess Pyrolyzate,” *Sixteenth Symposium (International) on Combustion, The Combustion Institute*, pp.1329, 1978.